2016

The Effects of Carbon Nanotubes on Cells in a Synthetic Oxygen Carrier Enriched Alginate Scaffold

Joshua Paul Tate
Louisiana State University and Agricultural and Mechanical College

THE EFFECTS OF CARBON NANOTUBES ON CELLS IN A SYNTHETIC OXYGEN CARRIER ENRICHED ALGINATE SCAFFOLD

A Thesis

Submitted to the Graduate Faculty of the
Louisiana State University and
Agricultural and Mechanical College
in partial fulfillment of the
requirements for the degree of
Master of Science in Biological and Agricultural Engineering

in

The Department of Biological and Agricultural Engineering

by
Joshua Tate
B.S., Louisiana State University, 2012
May 2016

ACKNOWLEDGEMENTS

I would like to thank Louisiana State University and the Biological and Agricultural Department for aiding in this research. I would also like to thank my research committee, Dr. Daniel Hayes, Dr. Steven Hall, Dr. Todd Monroe, and also Dr. Jeffrey Gimble for mentoring me and empowering me to further my education. I am also very appreciative of my fellow graduate students and the student workers within the Hayes-Monroe Labs. I would also like to thank my parents Delvin and Stephanie Tate for their support and encouragement; my fiancé, Syndney Jenkins, for the love, support, and sacrifices you made for me; and my sister, Toccara Sept, for all of your support through this journey.

TABLE OF CONTENTS

ABSTRACT

Huge progress has been made in the development of three dimensionally printed tissue structures. With the use of cells, three dimensional printers, and CAD drawing software, donor identical structures can be fabricated. However, cell scaffolds currently lack significant mechanical integrity which can result in reduced cellular survival, attachment, and nutrient delivery. For this reason, multiple strategies have been developed to increase and improve mechanical stability within engineered constructs without having to sacrifice cell viability.

The hypothesis of this paper was that incorporating Perfluorotributylamine (PFTBA), a greenhouse gas, with single walled carbon nanotubes (SWCNT), a allotrope of carbon with a cylindrical nanostructure, into an alginate scaffold will not only increase mechanical integrity but also cell survival. The following objectives were proposed: 1. Fabricate and characterize cell laden scaffolds of alginate and 2. Assess the addition of perfluorotributylamine and various concentrations of carbon nanotubes inside of cell laden scaffolds of alginate. Three configurations of perfluorotributylamine and carbon nanotubes were explored in an effort to maximize mechanical properties and cytocompatibility. Perfluorotributylamine was combined with gelatin from bovine skin and phosphate buffered solution to form a PFTBA emulsion. This emulsion was added to each alginate scaffold to encompass 5% of the entire alginate scaffold. Single walled carbon nanotubes were added in increasing concentrations to have four scaffolds, one control, 0 μg/ml, .1 μg/ml, and 1 μg/ml. The results of this study indicate that the configuration of 5% PFTBA emulsion + 1 μg/ml SWCNT + alginate, provided the best cell viability results; Picogreen fluorescence of 8532, excellent viability in live/dead stain, and sufficient morphological features while the control scaffold, containing alginate only, provided the best mechanical properties after a 7 day period. The results contradict the hypothesis that mechanical properties will increase with increasing SWCNT concentration, but support the hypothesis of improved cell viability with the incorporation of PFTBA emulsion to increasing SWCNT concentration.

1. INTRODUCTION

1.1 Overview of Thesis

The first chapter introduces the history of three dimensional printing and its modification to the process of bioprinting living cells. It mentions research into currently used engineered scaffolds and its application in organ transplantation surgeries. Chapter 2 reviews recent literature for the currently used hydrogels with their advantages and disadvantages, the chosen hydrogel used in this research, the additives used with the intention of increasing cell viability and mechanical properties. Chapter 3 details the in vitro three dimensional print fabrications and analysis of the various scaffold configurations. Chapter 4 concludes this thesis and provides direction for future research to better the development of engineered scaffolds.

1.2 History of Three Dimensional Printing

The idea of mass replication and production has been around for many centuries. With recent advancements in technology over the last couple of years, additive manufacturing has transformed from the production of two dimensional shapes into that of three dimensional. Rapid production of three dimensional shapes helped to increase the production speed of various products such as jewelry, electronics, and plastics in various industries such as automotive, aviation, and manufacturing. [1] In 1986, Charles W. Hull first depicted three dimensional (3D) printing as a method, deemed stereolithography, where thin layers of material were consecutively printed to form a solid three dimensional structure that was cured with ultraviolet light. [2] This process was later modified to create sacrificial resin molds that would form three dimensional scaffolds from biological materials. [1]

1.3 Three Dimensional Bioprinting

Bioprinting is a computer-aided manufacturing technique that allows the construction of structures layer by layer using biological materials, biochemicals, and living cells, with spatial control of functional components. [1] A bioprinter is constituted of a computer-aided positioning and deposition system, a bioink that feeds the deposition system, and a biopaper that acts as the substrate for the deposition. The computer controls the placing apparatus by moving the sample or the deposition heads along a predetermined path, initiating the deposition of the bioink when needed. Bioprinting is based on three approaches which include; biomimicry, autonomous self-assembly, and mini tissue building blocks. [1] Biomimicry involves the manufacturing of identical reproductions of the cellular and extracellular components of a tissue or organ. [3] In order to achieve biomimicry, distinct cellular functional components must be duplicated on a microscale. An understanding of the microenvironment, including the specific arrangement of functional and supporting cell types, gradients of soluble and insoluble factors, and composition of the extracellular matrix (ECM) is needed. [1] Autonomous self-assembly uses embryonic organ development as a guide. This approach relies on the cell as the primary driver of histogenesis, directing the composition, localization, functional, and structural properties of the tissue. [4, 5] The last approach, mini tissues can be fabricated and assembled into larger tissues by driven design, self-assembly, or a

combination. There are two strategies within mini tissues, self- assembling cell spheres which are assembled into large tissue and accurate, high-resolution reproductions of a tissue unit which are designed and then allowed to self-assemble into larger tissue. [6,7,8,9] Fabrication of these 3D biological structures are manufactured using various types of micro-extrusion printers, computer aided design software, and mathematical modeling to collect and digitize the complex tomographic and architectural design of the proposed tissue structure. Current bioprinting technologies are divided into three types of printers, which are, inkjet, microextrusion, and laser-assisted.

1.3.1 Microextrusion Bioprinter

Microextrusion bioprinters are the most common and affordable of the three types. These printers are more commonly used in personal and academic institutions with higher quality industrial versions that offer better resolution, speed, and spatial control. [10] Microextrusion bioprinters have been used to fabricate various tissue types, such as, aortic valves, branched vascular trees, as well as tumor models [1]. Material is deposited in continuous beads of material rather than liquid droplets. The three types of microextrusion bioprinters are pneumatic, piston, and screw dispensing systems, the last two of which are deemed mechanical. [11, 12, 13] Pneumatic dispensers are advantageous due to simpler drive-mechanism components, with the force limited only by the air-pressure capabilities of the system, suited to dispense high-viscosity materials. One disadvantage includes less control of flow due to the delay of the compressed gas volume. Mechanical dispensing systems have smaller and more complex components which offer more spatial control over the material flow, and are thought to be beneficial for the dispensing of hydrogels with higher viscosities. [14] These benefits often result in reduced maximum force capabilities.

The main advantage of microextrusion bioprinting technology is the ability to deposit very high cell densities. Achieving physiological cell densities in tissue-engineered organs is a major goal for the bioprinting field. Cell viability after microextrusion bioprinting is in the range of 40–86%, depending on extrusion pressure and nozzle gauge. [15,16] Use of improved biocompatible materials, such as hydrogels, that are mechanically robust during printing and that develop secondary mechanical properties after printing can improve cell viability and function after the printing process. [17, 18]

1.4 Engineered Scaffolds

Tissue engineering aspires to devise ways to artificially produce organs and tissue structures in the human body. In 3D printing, layer by layer precise positioning of biological materials, biochemical and living cells, with spatial control of the placement of functional components, are used to fabricate 3D structures in the form of scaffolds. [1] The field of bioprinting also faces other challenges shared by all researchers in the fields of tissue engineering and regenerative medicine. The central challenge is to reproduce the complex micro-architecture of extracellular matrix (ECM) components and multiple cell types in sufficient resolution to repeat biological function. [1] Another challenge in the 3D bioprinting field has been to find materials that are not only compatible with biological materials and the printing process but can also provide the desired mechanical and functional properties for tissue constructs.

1.5 Description of the Need for Engineered Scaffolds

The most popular treatment for loss or damaged tissues and organs is organ transplantation. According to the U.S. Department of Health and Human Services (DHH), an average of 21 patient deaths occur each day waiting for transplants that cannot take place due to the shortage of donated organs. [19] Thus there is a significant need for improved techniques to combat the reproduction and repair of various organs as they fail or become obsolete. The concept of complete organ reproduction is in infancy however; the research surrounding producing a patient's own cells in the form of hydrogel scaffold is a stepping stone to reach this goal.

2. LITERATURE REVIEW

2.1 Hydrogels for Tissue Engineering

Drury et al. provides a thorough review of the various hydrogels used for tissue engineering applications. There are various strategies used to engineer tissues that depend on incorporating a material scaffold. These scaffolds are used to mimic the extracellular matrix so that cells can be distributed into a three-dimensional architecture to properly grow and form the intended tissue. [20] In order to produce these scaffolds, a class of highly hydrated polymer materials with water content greater than 30% by weight deemed hydrogels, are being used. These hydrogels are made up of natural and synthetic hydrophilic polymer chains which have similar characteristics to tissues and ECM. [21] Selection between these two types of hydrogels is dependent upon several factors such as rate of gel formation, nutrient diffusion, and cell adhesion.

2.1.1 Synthetic hydrogels

The use of synthetic hydrogels in tissue engineering is due to their customizable chemistry and properties. Synthetic hydrogels can be manufactured with various molecular weights, chain linkages, and solidification methods which can factor into the material mechanical properties and formation methods. [20] Examples of such material include, PEO, PEG, PVA, and PLA.

2.1.2 Natural hydrogels

Natural hydrogels are polymers that are made up of components that are either a part of or have molecular properties similar to that of natural ECM. These materials include but are not limited to collagen, HA, alginate, and chitosan.

a Sodium Alginate

Alginate is non-biodegradable, bio-inert, and biocompatible material derived from brown seaweed and bacteria. It is a hydrophilic, linear polysaccharide of (1–4)-linked β-D-mannuronic acid (M) and α-L-guluronic acid (G) monomers which are distributed in either repeating or alternating blocks. [22, 23, 24] Alginate is normally combined with water or a saline to produce a solution which forms a gel when divalent cations such as Ca^{2+}, Ba^{2+}, or Sr^{2+} cooperatively interact with blocks of G monomers to form ionic bridges between different polymer chains. [22] Following cross linkage, Alginate undergoes a slow, uncontrolled dissolution with mass loss by ion exchange of calcium resulting in the dissociation of individual chains and loss of mechanical integrity.

A solution to this can greatly enhance cell viability and hydrogel life.[25] The most commonly used divalent cation with alginate is Ca^{2+}, normally used in the form of Calcium Chloride. Alginate has been proven to be a compatible material with a variety of uses including drug delivery, cell encapsulation, and in vivo which encourages its use in tissue engineering.

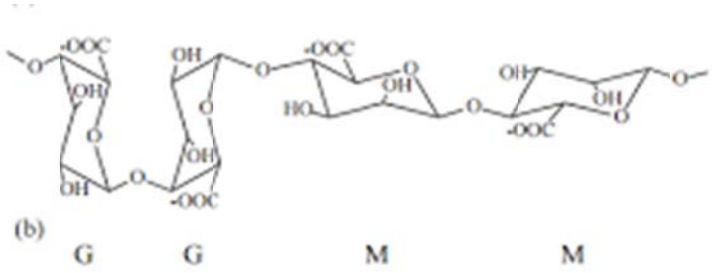

Figure 2.1**:** Structure of naturally derived alginate polymer. (Drury et al. 2003). Reprinted from Biomaterials, Vol 24, Jeanie L. Drury, David J. Mooney, Page 4340.

2.2 Addition of Carbon Nanotubes

One addition to the current alginate hydrogel composition is to add carbon nanotubes, which not only have been shown to improve mechanical properties, but also have aided in cell viability. Carbon nanotubes are sheets of graphite rolled into cylindrical shaped tubes. Carbon nanotubes (CNT) are highly porous as well as lightweight which provides a similarity to naturally occurring collagen fibers of the extracellular matrix. This similarity along with the size of the carbon nanotubes allows the ability to greatly influence cell adhesion, proliferation, and differentiation. [26] Carbon nanotubes can be divided into two categories based off of the diameter size, single walled carbon nanotubes (SWCNT) and multiple walled carbon nanotubes (MWCNT). Single walled tubes have a diameter between 0.8 and 2 nanometers, while multiple walled tubes show a diameter between 2 and 100 nanometers. [27,28] The flexible arrangement of the carbon atoms within the tubes gives them great mechanical strength with a Young's modulus of 0.27 - 1.34 TPa and a tensile strength between 11 - 200 GPa.[29,30] The incorporation of carbon nanotubes into a polystyrene polymer showed a 36-42% elastic modulus increase and a 25% tensile strength increase. [31] A composite of single walled carbon nanotubes and poly-L-lactide (PLLA) showed a 12% increase in tensile strength and a reduced rate of degradation. [32] Increases in the tensile strength, reduced rate of degradation, and elastic modulus, among other structural modifications, are beneficial when developing structural tissues and organs such as bone, as a hydrogel scaffolds needs to degrade at a rate that will also support cell growth and formation of tissue. [33,34,35] A study performed showed that the formation of hydroxyapatite crystals, the largest mineral component of natural bone, on SWCNTs and MWCNTs were almost identical to osteoblasts cultured on woven bone. Most interestingly, cells grown on SWCNTs, which are similar in size to the triple helix collagen fibers of natural bone, had diameters mirroring those from natural osteoblast size. [36] SWCNTs have various uses in many tissue engineering with research on them taking place in mesenchymal stem cells and neural tissue engineering. SWCNTs aligned on glass substrates, by centrifugal forces, compared to randomly oriented SWCNTs showed a 120% increase in mesenchymal stem cells (MSCs) proliferation.[37] Neuronal cells grown on SWCNT multilayer films showed stimulated nerve repair. [38] In doses of 0.1 and 1μg/ml, surface markers and viability of human adipose stem cells showed increases compared to 10, 20, 50, and 100 μg/ml after a 7 day period. [39, 40]

With the incorporation of carbon nanotubes into alginate hydrogels, cell viability and proliferation could be increased and the mechanical structure of these constructs could be greatly extended and potentially strengthened. This concept should be further explored as a method for newly printed tissue constructs.

2.2.1 Carbon Nanotube Functionalization

Carbon nanotubes are naturally chemically inert and dispense unevenly in various polymers. In order to improve biocompatibility and increase the ability to disperse evenly, functionalization is required in order to incorporate carbon nanotubes into polymers. [41] Functionalization normally involves the addition of carboxyl or alcohol groups to the ends of the nanotubes. The bonds formed between the carbon nanotubes and functional groups are useful in tissue engineering because they are weak enough to allow various reactions to take place within the biochemical environment, but not too weak to prevent rapid chemical decay.[42,43] Similar to size, functional groups can have an effect on cell growth and differentiation. Charged carboxyl groups have shown increased chondrocyte growth and ECM protein expression. [44] Recent results also have shown that when functionalizing carbon nanotubes with nitric and sulphuric acids, functionalization periods of 5 hours compared to .5 hours, increase cell viability. [45]

2.3 Perfluorocarbons

Perfluorocarbons (PFCs) are nonaqueous, cytocompatible, and highly oxygenated fluids. These hydrocarbons have fluorine substituted in place of most or all hydrogen atoms, an increased molecular mass, and also specific gravities twice that of water. [46] Due to the carbon to fluorine bond strength, 487 kJ mol^{-1}, PFCs have noteworthy chemical and thermal stability, great spatial arrangement, and the ability to dissolve large quantities of respiratory gases [46]. These solutions have been previously used in research by Clark and Gollan to test and confirm the survival of small mice fully submerged in fluorobutyltetrahydrofuran. [46] More recently, research has shown that the incorporation of these solutions with bioreactors and cell cultures resulted in higher cell proliferation and cell bioproduct assembly. Various studies using PFC emulsions have also been conducted for use in preserving human and animal organs before transplantation. [47, 48]

2.3.1 Addition of Perfluorotributylamine

Perfluorotributylamine (PFTBA) is a type of perfluorocarbon useful with cell and organ printing due to its inert properties. Perfluorotributylamine has a density of 1.88 g cm^{-3}, approximately twice the density of water. [49] One of the ideal benefits of Perfluorotributylamine is that is hydrophobic, which makes it non-miscible leading to aided mechanical support of printed scaffolds during the three dimensional fabrication process. Campos et al previously conducted study where stem cell laden agarose hydrogel scaffolds were printed a Perfluorotributylamine solution. Results showed excellent improvement in compressive strength, excellent cell viability after 24 hours and 21 days, and increased cell proliferation using stem cells.

Studies have also demonstrated the use of a PFTBA emulsion, composed of PFTBA, lecithin, and Phosphate Buffered Saline, increasing oxygen levels within cellular scaffolds which in turn increase gene expression, cell viability, nerve cell regeneration, osteogenic differentiation, and bone formation in vivo. [50, 51, 52]

2.4 Future Work

From this review, alginate hydrogel, carbon nanotubes, and PFTBA, all commonly used in tissue engineering were presented and reviewed. During this process of examining the many benefits in cell viability and mechanical integrity of these materials, more research will need to be done to show appropriate configurations and concentrations of these materials in vitro and in vivo. More extensive lab trials and animal trials, which will eventually lead to human trials, will need to be done to provide the date for clinical use.

2.5 Conclusion

The use of alginate hydrogels, carbon nanotubes, and PFTBA, have had notable occurrences in laboratory use and all have a potential to be further developed for clinical use in the field of tissue engineered scaffolds. As the need for organ transplants is increased, the need for alternatives to shortages will continue to rise. Due to the revolutionary advancements in technology and medicine, there has never been a better time to continually improve the current knowledge of three dimensionally printed biological scaffolds. This search for improvement has led to many additives being experimented with to research if they are able to improve the biological properties of current hydrogel solutions. These additions to current hydrogel configurations have led to many developments in aiding three dimensionally printed organ developments, improved mechanical strength of scaffold models, improved cellular viability and proliferation, and increased knowledge of tissue engineering. The additives reviewed here have led to bettering the current understanding of three dimensional scaffolds and additives for tissue engineering experiments. With further research on the combinations of these materials in vitro, in vivo, and clinically, much advancement within the field are on the horizon.

3. IN VITRO EVALUATION OF THREE DIMENSIONALLY PRINTED PERFLUOROTRIBUTYLAMINE AND CARBON NANOTUBE ENRICHED ALGINATE SCAFFOLD

3.1 Project Purpose

Due to the large number of organ transplant surgeries occurring each year and with these procedures projected to increase, there is a need to discover a more effective alternative to organ transplantation. The idea of customizable, patient exact organ production is a novel concept currently being worked towards through three dimensional printing, hydrogels, and human cells and their production to form tissue engineered scaffolds. There is a need for researchers to become more efficient and gain better control over the production process, especially regarding cellular viability and mechanical stability. Current research has shown that these scaffolds lack in mechanical integrity and life of implanted cells. Poor mechanical integrity can result in poor gas exchange and can even play a factor in reduced viability of implanted cells. This study explored several compositions of single walled carbon nanotubes and a emulsion made with perfluorocarbon, phosphate buffered saline and gelatin from bovine skin. The 5% PFTBA emulsion + 1 µg/ml SWCNT + alginate, provided the best cell viability results; Picogreen fluorescence of 8532, excellent viability in live/dead stain, and sufficient morphological features while the control scaffold, containing alginate only, provided the best mechanical properties. This composition may have application as an improvement with hydrogels and could be further explored.

3.2 Materials and Methods

Sodium Alginate and Calcium Chloride (Sigma Aldrich, U.K.) were treated with ultraviolet (UV) light for sterilization three times for a 30-minute cycle each time. UV-sterilized sodium alginate was dissolved in sterile Phosphate Buffer Saline (PBS) to make 2% (w/v) solutions. Similarly, the crosslinking solution was prepared by dissolving UV-sterilized Calcium Chloride particles in sterile Dulbecco's Modified Eagle Medium (DMEM) supplemented with 10% fetal bovine serum (FBS) and 1% triple antibiotic achieving 4% (w/v). Solutions were mixed with a magnetic stirrer at room temperature until homogeneity was reached. To eliminate any remaining contaminant, both solutions were passed through a filter with a pore size of 0.22 µm.

3.2.1 Carbon nanotube Functionalization

Single Walled Carbon Nanotubes were obtained in powder form from US Research Nanomaterials, Inc. (Stock#: US 4110) with average diameter 1.1 nm and a length of 5- 30 µm. The purity of SWCNTs used was >90%. 30 mg of pure SWCNTs was dispersed in 60 mL of 1:3 mixture of 98% nitric acid (HNO3) and 70% sulfuric acid (H2SO4) in a round bottom flask equipped with a condenser and refluxed for 180 minutes at 120°C while stirring at a rate of 500 rpm as shown in figure 3.1. [45]

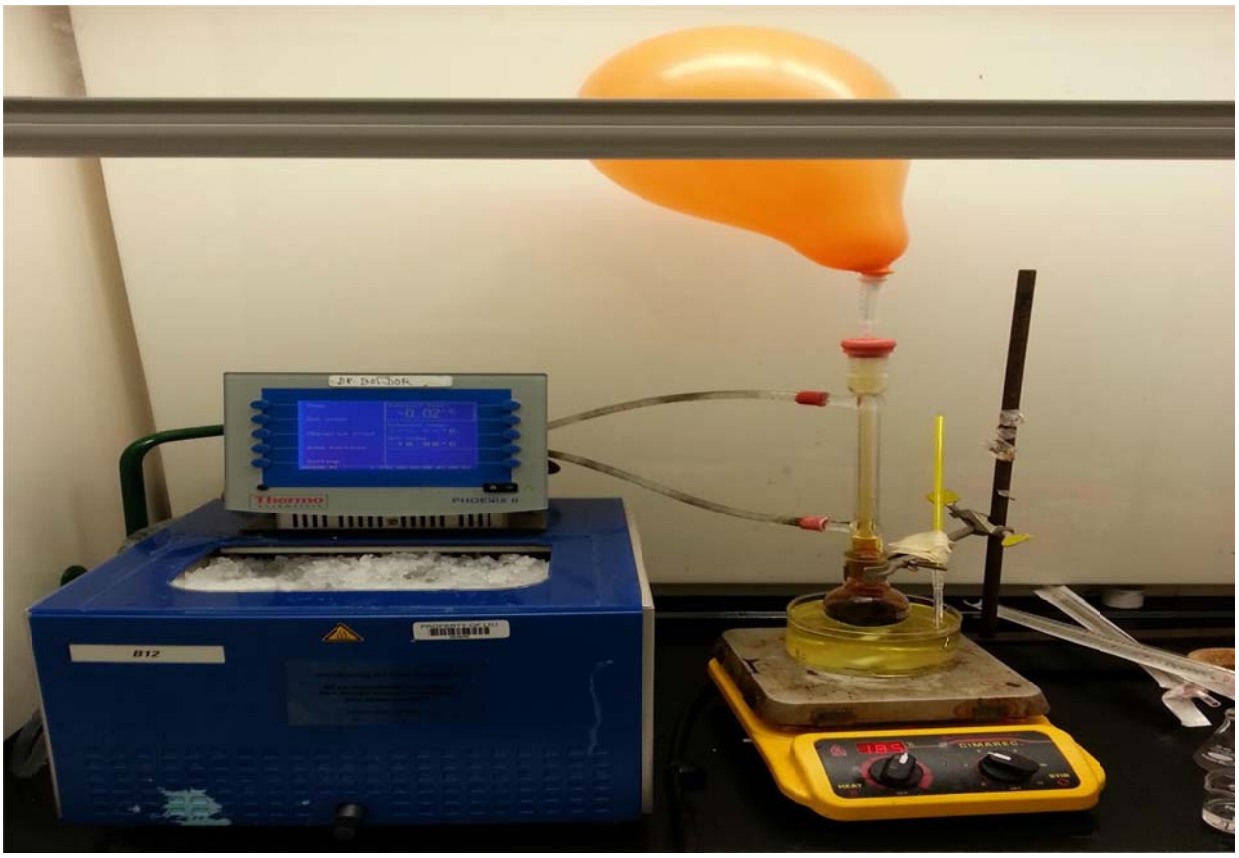

Figure 3.1: SWCNT functionalization set up including water bath, condenser, flask, oil bath, hot plate, balloon, and thermometer.

Next, the acid-treated SWCNTs were centrifuged for 10 minutes at 2400 × g and sonicated for 1 hour with water in sonicator exchanged every 20 mins to prevent overheating. The SWCNTs were washed extensively in 1200 ml of deionized water until a constant pH value in the range of 5–6 was attained and was collected on a .22 µm filtering membrane. The SWCNTs were then washed with PBS to achieve a pH of 7. Finally, the SWCNTs were washed off of the membrane into 6, 50 ml centrifuge tubes, frozen using liquid nitrogen, and dried inside a vacuum chamber over two days at 80 °C. The resulting functionalization of the SWCNTs was determined by Fourier Transform Infra-Red (FTIR) spectroscopy using potassium bromide plates. Previous research has shown that successful attachment of the carboxyl group is evident by a peak in the absorbance around between 1700 cm^{-1} and 1750 cm^{-1}, as shown in figure 3.2, which shows the unfunctionalized single walled carbon nanotubes and figure 3.3 which shows the functionalized single walled carbon nanotubes.

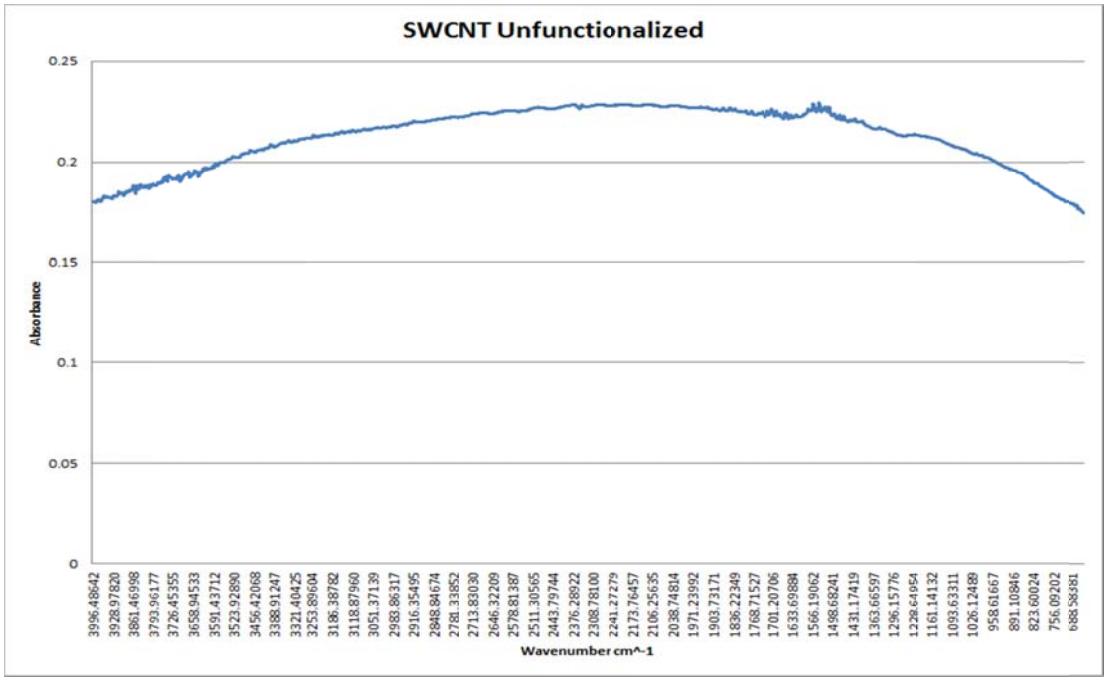

Figure 3.2: Absorbance vs Wavenumber display of unfunctionalized single walled carbon nanotubes.

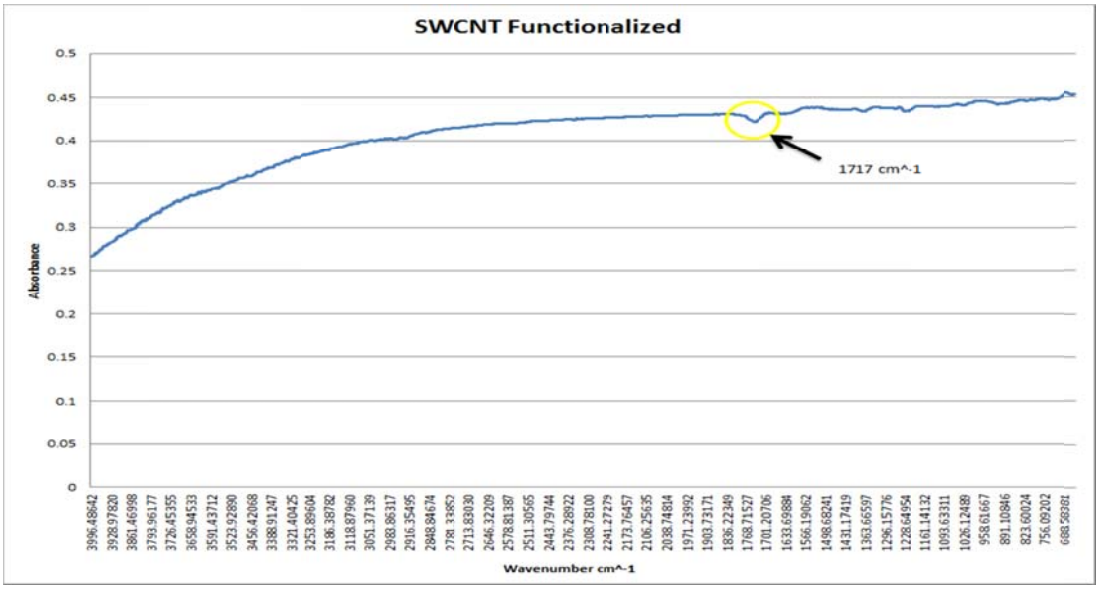

Figure 3.3: Absorbance vs Wavenumber display of functionalized single walled carbon nanotubes. Inverse peak around 1717 cm^{-1} confirms successful attachment of carboxyl groups to single walled carbon nanotubes.

3.2.2 Dispersion of Carbon Nanotubes

The preparation of carbon nanotubes in Dulbecco's Modified Eagle Medium (DMEM) supplemented with 10% fetal bovine serum (FBS) and 1% triple antibiotic used a sonication/centrifugation protocol described by Chin et. al. [53] Briefly, 1 mg of functionalized SWCNT powder was dispensed into an Eppendorf tube containing 1 ml of DMEM/FBS, vortexed for 1 min and sonicated for 10 min at 0 degrees Celsius. The resulting suspension was centrifuged in an Eppendorf tube for 2 minutes at 16,000 g. The supernatant was carefully recovered to produce a DMEM-SWCNT dispersion.

3.2.3 Perfluorotributylamine Emulsion Preparation

A PFTBA emulsion was prepared in the following manner. 95 mg of gelatin from bovine skin and 400 µL PFTBA was added to 600 µL of phosphate buffered solution.[50, 51, 52] The solution was sonicated at 4 °C twelve times for 15 seconds with a 1 minute interval between each sonication.

The mixture was then reheated in a water bath of 37 °C and vortexed before usage. The PFTBA emulsion was sterilized by filtering through a .22 µm membrane filter and treated with UV light for sterilization three times for a 30-minute cycle each time.

3.2.4 Cell Culture

NIH 3T3 mouse fibroblast from passages 14 to 27 were cultured in Dulbecco's Modified Eagle Medium (DMEM) supplemented with 10% fetal bovine serum (FBS) and 1% triple antibiotic in 25 cm^2 tissue culture flasks. All cells were incubated at 37°C and 5% CO_2. The media was changed in each flask every 3 days and passaged at 80% confluence.

3.2.5 Scaffold Fabrication

Mouse fibroblast cells were resuspended at 250,000 cells/ml in 2% sodium alginate by vortexing for 10-20 seconds. Alginate with Mouse fibroblast cells was taken into 20ml syringes and passed through medical tubing to a 20 gauge needle tip. 4% Calcium chloride was also taken into a 20 ml syringe passed through medical tubing to a 22 gauge needle. Both of which were attached to a custom 3D printed face of the Reprappro Mendel 3D printer. The Alginate solution syringe was controlled by the extruder motor of the printer which was attached to a syringe extruder. This allowed for the control of the printing material directly from the printer. The calcium chloride solution was extruded at an angle so as to drip down the needle of the alginate. The extrusion was controlled by an external syringe pump that was set to 70 ml/h. A 5 mm tall, 4 mm diameter cylinder structure was created using a SolidWorks which was then converted to g- code through the software Slic3r. The g-code was then loaded to Pronterface. Scaffolds were printed in various configurations, incubated for 7 days with media exchanged 3 days after print, and tested. The control scaffold contained no carbon nanotubes and no PFTBA emulsion. The remaining 3 scaffolds were printed with increasing amounts of carbon nanotubes starting at 0 µg/ml to .1 µg/ml and lastly 1 µg/ml with a 5% v/v addition of PFTBA emulsion. Scaffolds were printed in triplicates for each experiment.

Table 1: Scaffold Configurations

	Control Scaffold	**Scaffold 1**	**Scaffold 2**	**Scaffold 3**
Carbon nanotubes	0 µg/ml	0 µg/ml	.1 µg/ml	1 µg/ml
PFTBA Emulsion	0 %	5 %	5 %	5 %

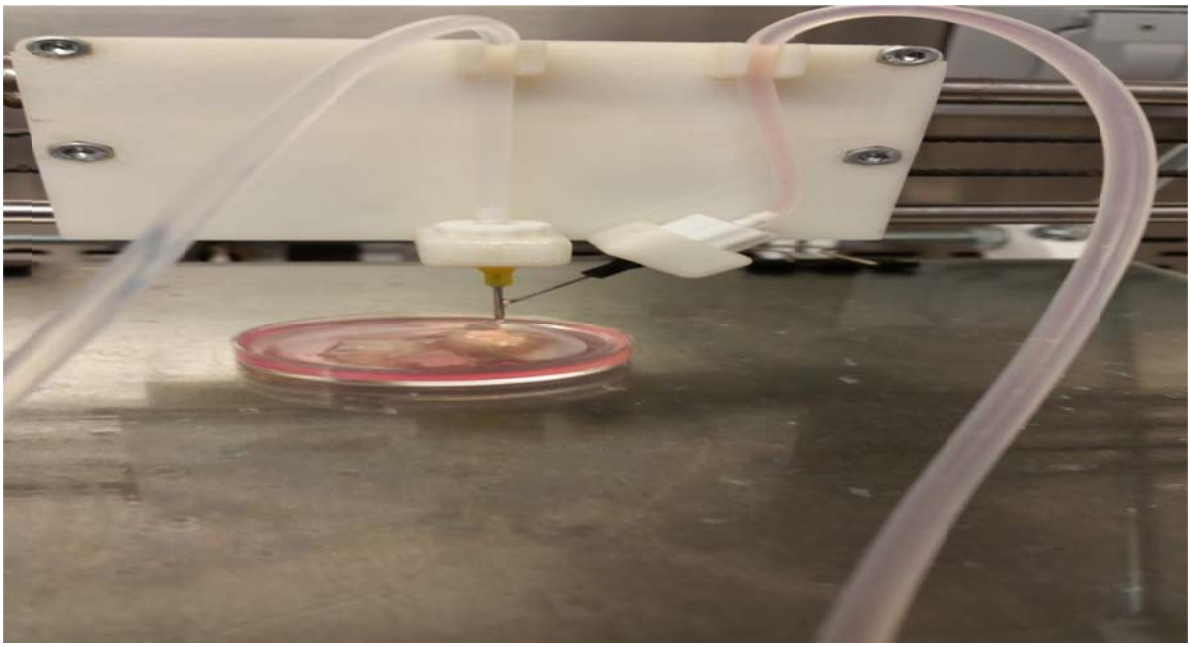

Figure 3.4: Scaffold fabrication process illustrating the extrusion of the various alginate hydrogel configurations and the calcium chloride angled drip method to solidify the scaffold structures.

3.3 Cell Viability Studies

3.3.1 Live/Dead Assay

The 3D cell laden hydrogels were incubated under controlled conditions for 7 days. The live/dead assay was created using 20µL of EthD-1, 10ml D-PBS, and 5µl calcein AU. The prints were moved to a 48 well plate and covered with solution. Images were taken using a lumar-stereo microscope.

3.3.2 Picogreen

The printed structures were incubated and put on a rocker with proteinase K at 56˚C overnight. 50µl of the solution with 50µl of Picogreen dye were migrated to a 96 well plate. The samples were exposed to 480nm light, and the total DNA concentration was compared to each other.

3.4 Cell Morphology Studies

3.4.1 F.Actin Stain

The printed structures were rinsed with PBS, fixed with 4% paraformaldehyde for 20 minutes, and rinsed again with PBS. Next the scaffolds were permeabilized with 0.1% triton x-100 for 10 minutes and lastly stained with ActinGreen 488 reagent for 30 mins. Following the process, the stain was removed; the scaffolds were rinsed with PBS and imaged using a confocal microscope.

3.5 Mechanical Analysis

Compression testing was performed at room temperature on the structures each being 8mm diameter and 10mm in height. This was done using a hydraulic universal testing machine (MODEL) using an extension rate of 1 mm min^{-1}.

3.6 Statistical Analysis

All results were expressed as a mean ± percent error.

3.7 Results

3.7.1 Live/Dead Stain

To analyze the 3D scaffolds with respect to cell viability. Mouse fibroblast cells were seeded at a density of 250,000 cells per milliliter. The cell images for the mouse fibroblast cells revealed excellent cell viability 7 days after the printing process and incubation period. As shown if figures 3.5, 3.6, 3.7, and 3.8

Control:

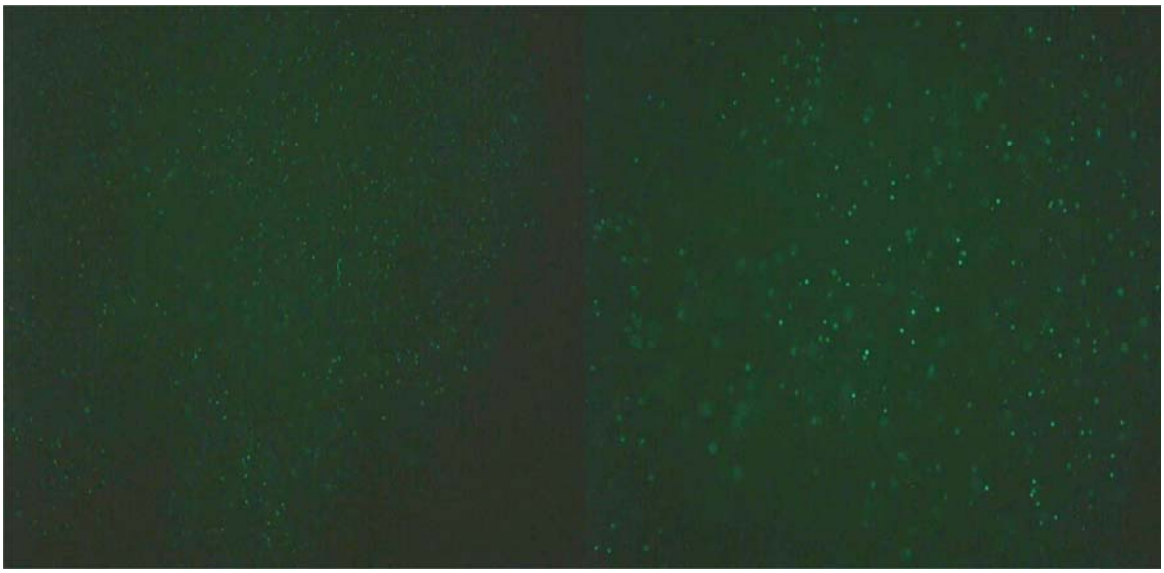

Figure 3.5: Live/dead Control staining showing viable 3T3, 7 days after being printed.

5% PFTBA Emulsion:

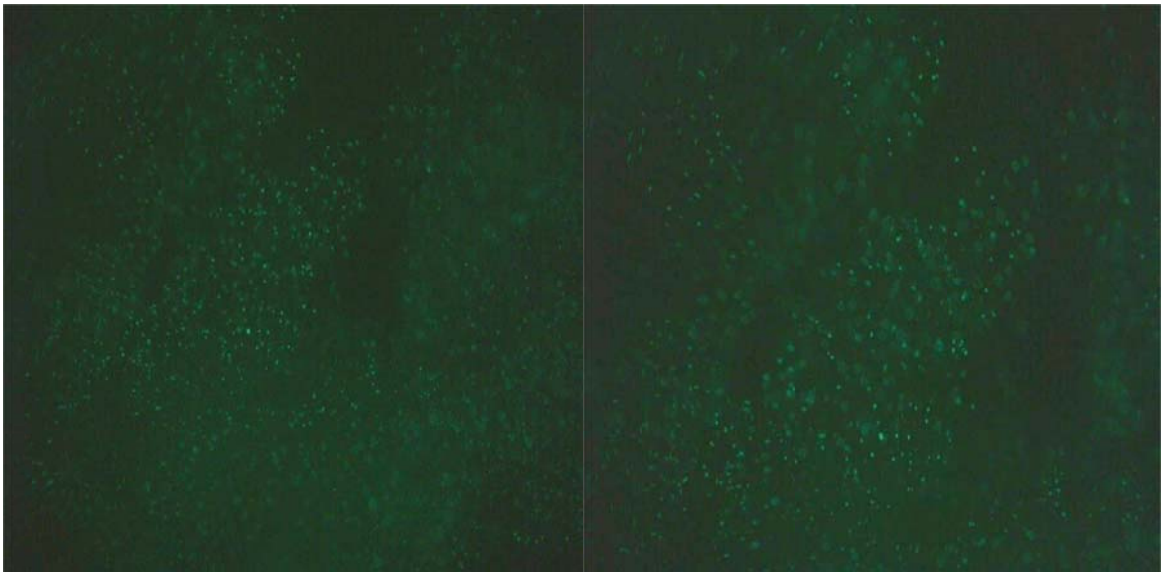

Figure 3.6: Live/dead 5% PFTBA Emulsion staining showing viable 3T3, 7 days after being printed.

.1 µg/ml Carbon Nanotubes; 5% PFTBA Emulsion:

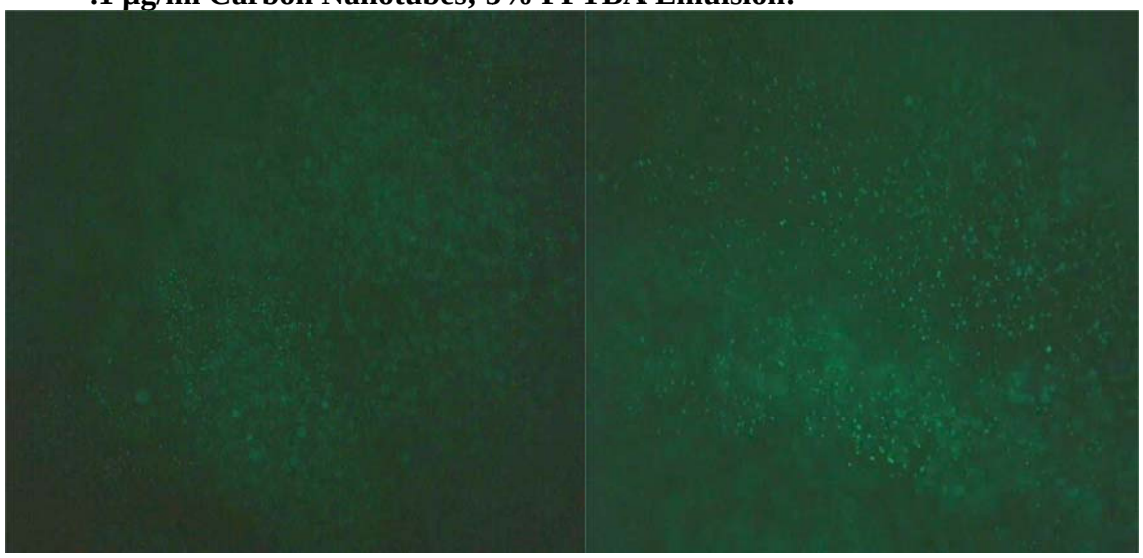

Figure 3.7: Live/dead .1 µg/ml Carbon Nanotubes; 5% PFTBA Emulsion staining showing viable 3T3, 7 days after being printed.

1 µg/ml Carbon Nanotubes; 5% PFTBA Emulsion:

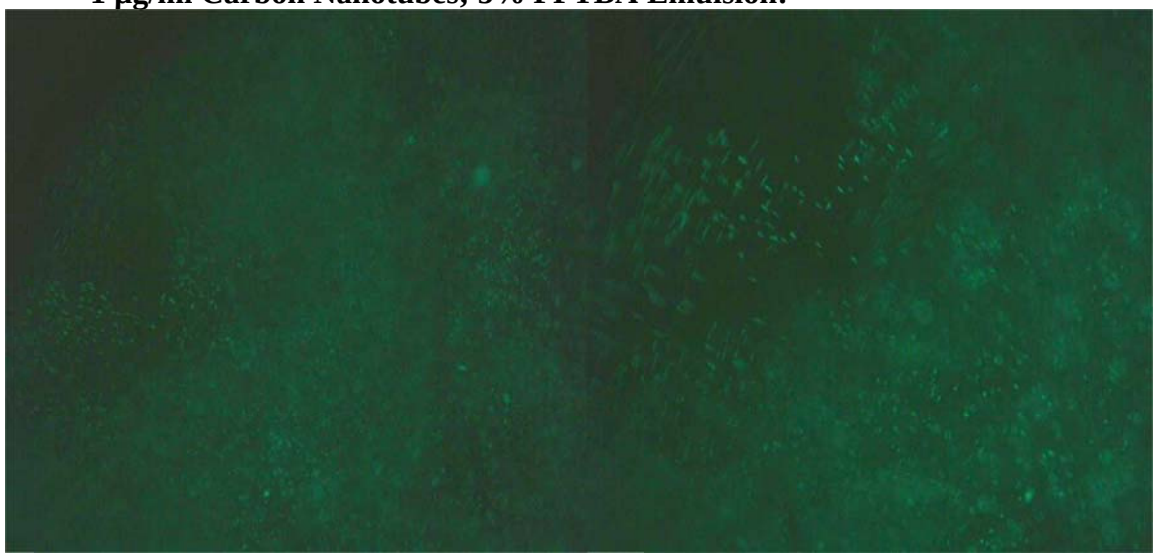

Figure 3.8: Live/dead 1 µg/ml Carbon Nanotubes; 5% PFTBA Emulsion staining showing viable 3T3, 7 days after being printed.

3.7.2 Picogreen

For samples undergoing fluorescence analysis, a cell concentration of 250,000 cells per milliliter was used. The numerical value of the fluorescence tends to directly correlate to the numerical value of the actual number of cells counted within each scaffold structure. The Picogreen begins with an average of fluorescence of 2611 and increases to 4965, 5370, and 8532, for the controls, 5% PFTBA emulsion scaffolds, .1 µg/ml, and 1 µg/ml scaffolds, respectively, as shown if figure 3.9. The fluorescence activity shown in the chart below, of the mouse fibroblast cells, tends to increase from the control scaffolds to those with no carbon nanotubes and a 5% pftba emulsion, to those with increasing amounts of carbon nanotubes, .1 µg/ml and 1 µg/ml, with a 5% pftba emulsion. Statistically speaking, there was a 90.157% increase between the control scaffolds and the scaffolds containing a 5% pftba emulsion. There was an 8.157% increase between the scaffolds containing a 5% pftba emulsion and those containing a 5% pftba emulsion and .1 µg/ml carbon nanotube concentrations. Lastly, there was 58.883% increase between the scaffolds containing a 5% pftba emulsion and .1 µg/ml carbon nanotube concentrations and those containing a 5% pftba emulsion and 1 µg/ml carbon nanotube concentrations.

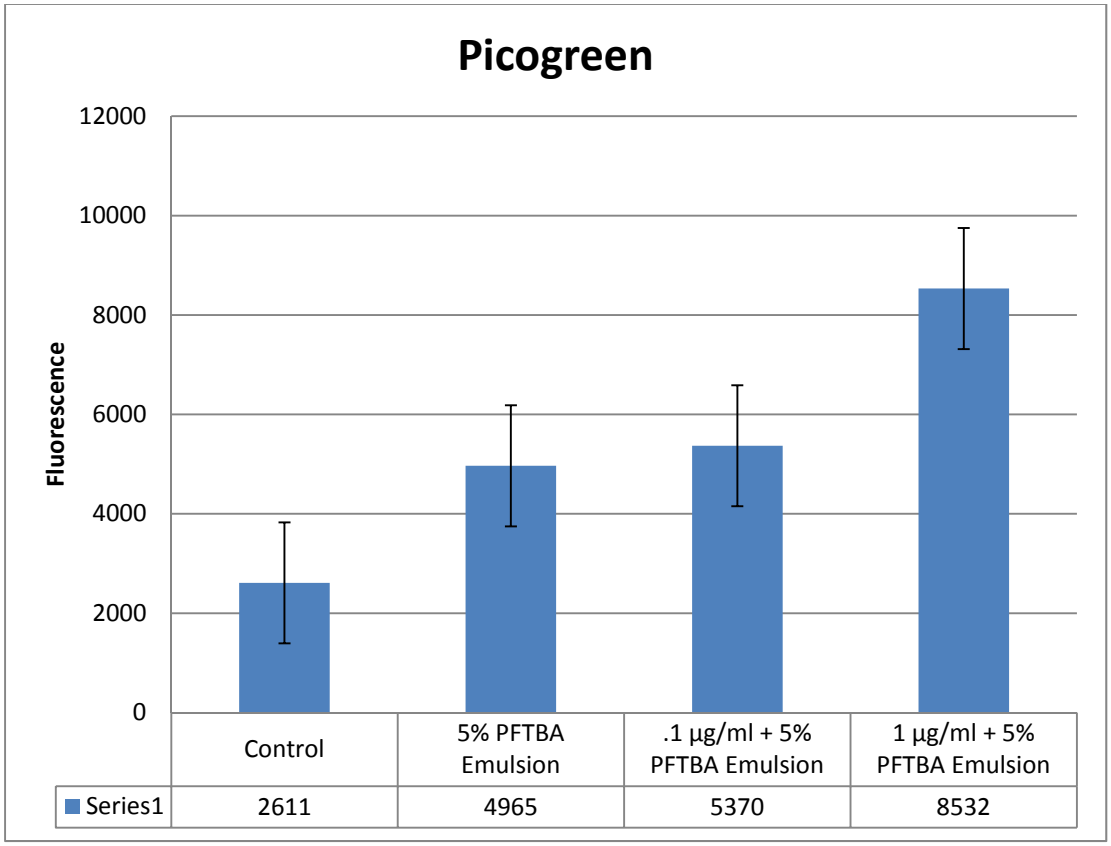

Figure 3.9: Fluorescence of 3T3 laden hydrogels after 7 days.

3.7.3 F.Actin Stain

To analyze the 3D scaffolds with respect to cell viability. Mouse fibroblast cells were seeded at a density of 250,000 cells per milliliter. The cell images for the mouse fibroblast cells revealed cell morphology unique to those commonly found to normal mouse fibroblast cells for all of the various scaffold configurations. As shown in figures 3.10, 3.11, 3.12, and 3.13.

Control:

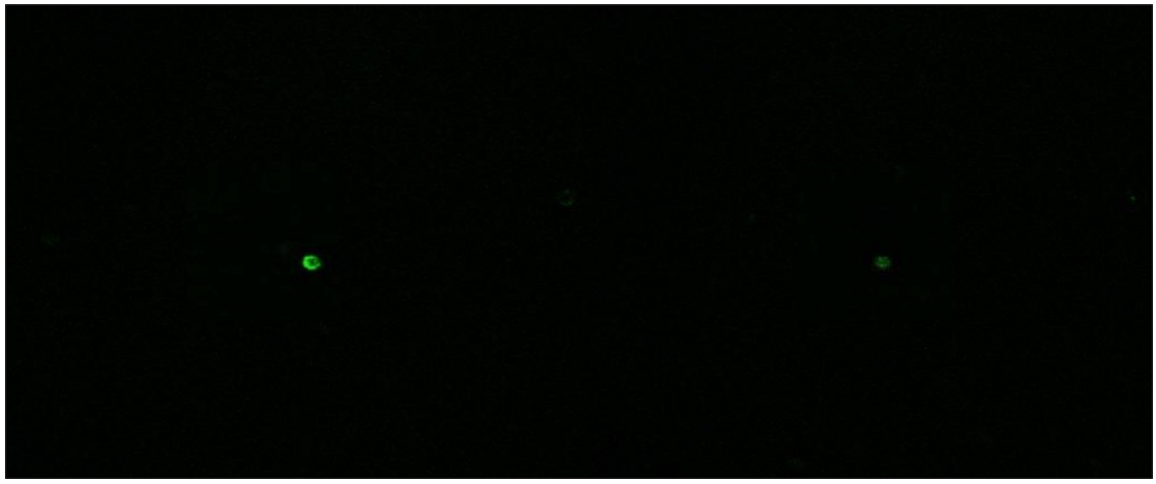

Figure 3.10: F.Actin Control staining showing cell morphology of 3T3, 7 days after being printed.

5% PFTBA Emulsion:

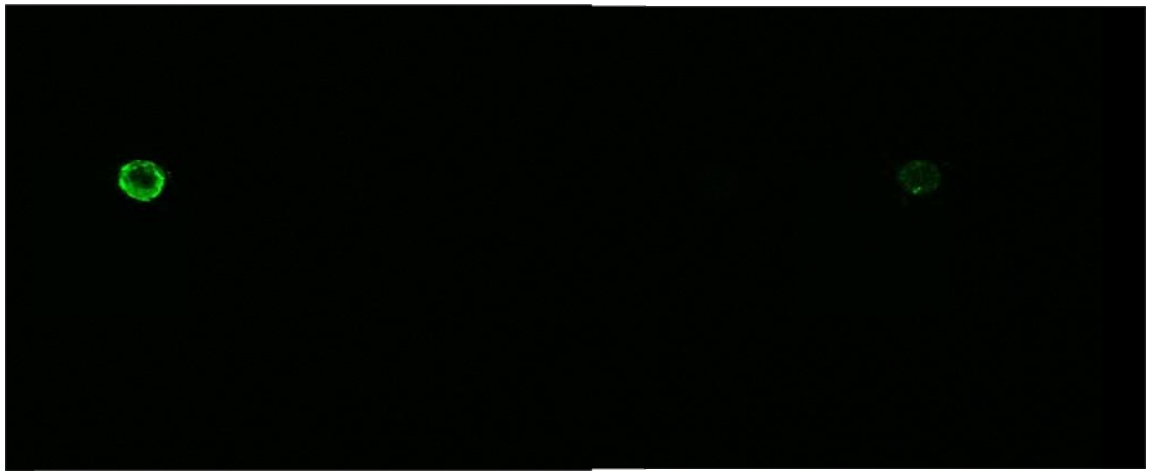

Figure 3.11: F.Actin 5% PFTBA Emulsion staining showing cell morphology of 3T3, 7 days after being printed.

.1 µg/ml Carbon Nanotubes; 5% PFTBA Emulsion:

Figure 3.12: F.Actin .1µg/ml Carbon Nanotubes; 5% PFTBA Emulsion staining showing cell morphology of 3T3, 7 days after being printed.

1 µg/ml Carbon Nanotubes; 5% PFTBA Emulsion:

Figure 3.13: F.Actin 1µg/ml Carbon Nanotubes; 5% PFTBA Emulsion staining showing cell morphology of 3T3, 7 days after being printed.

3.7.4 Mechanical Analysis

The printed scaffolds were seeded with cells at a density of 250,000 cells per milliliter. Three scaffolds of each type were evaluated 7 days after print. The three specimens were tested at a rate of 1 mm per minute using a 2 kN load cell.

The tests were performed at room temperature. The mechanical tests revealed a vast difference in the stress, strain, and compressive strength between the control and combination scaffolds. The Young's Modulus begins with an average of 12,850 kPa and decreases to 2639, 2382, and 1609 kPa, for the controls, 5% PFTBA emulsion scaffolds, .1 µg/ml, and 1 µg/ml scaffolds, respectively, as shown in figure 3.14.

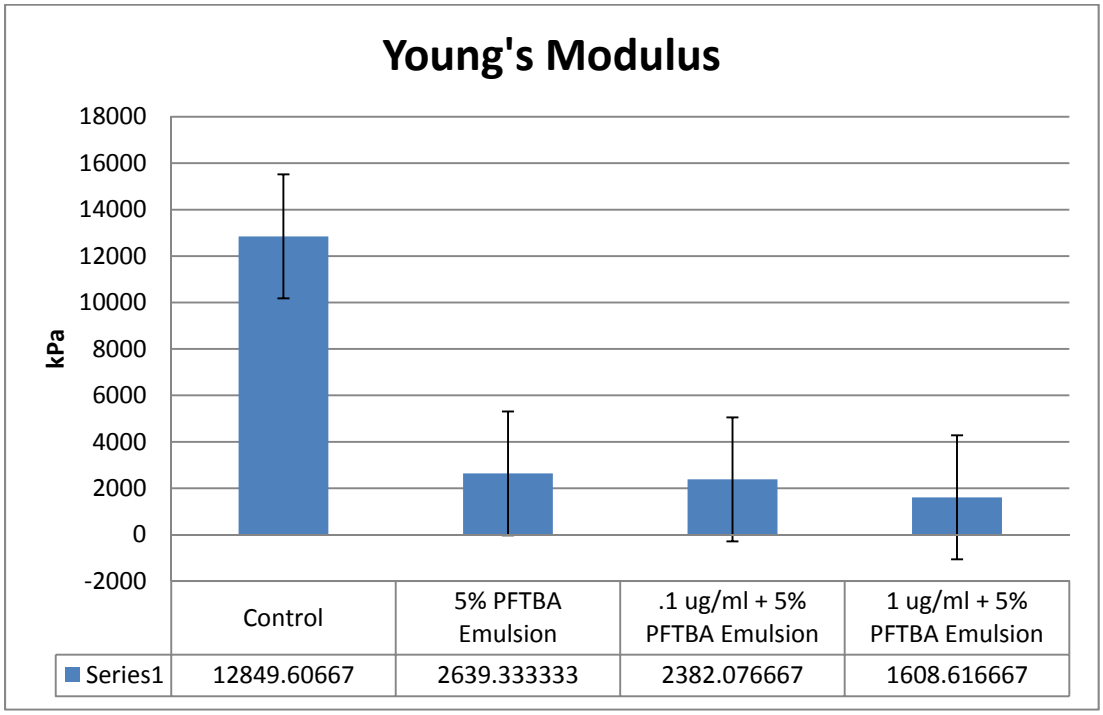

Figure 3.14: Young's Modulus of 3T3 laden hydrogels after 7 days. The control scaffold had significantly higher results than the remaining scaffolds. The remaining scaffolds decreased in results, with increasing concentration of SWCNTs.

Statistically speaking, there was a 79.459% decrease between the control scaffolds and the scaffolds containing a 5% pftba emulsion. There was a 9.747% decrease between the scaffolds containing a 5% pftba emulsion and those containing a 5% pftba emulsion and .1 µg/ml carbon nanotube concentrations. Lastly, there was 32.469% decrease between the scaffolds containing a 5% pftba emulsion and .1 µg/ml carbon nanotube concentrations and those containing a 5% pftba emulsion and 1 µg/ml carbon nanotube concentrations. The Compressive Stress at Tensile Strength begins with an average of 983 kPa and decreases to 302, 274, and 246 kPa, for the controls, 5% PFTBA emulsion scaffolds, .1 µg/ml and 1 µg/ml scaffolds, respectively, as shown if figure 3.15. Statistically speaking, there was a 69.313% decrease between the control scaffolds and the scaffolds containing a 5% pftba emulsion. There was a 9.102% decrease between the scaffolds containing a 5% pftba emulsion and those containing a 5% pftba emulsion and .1 µg/ml carbon nanotube concentrations.

Lastly, there was 10.462% decrease between the scaffolds containing a 5% pftba emulsion and .1 µg/ml carbon nanotube concentrations and those containing a 5% pftba emulsion and 1 µg/ml carbon nanotube concentrations. These results are most likely due to the incorporation of the PFTBA emulsion.

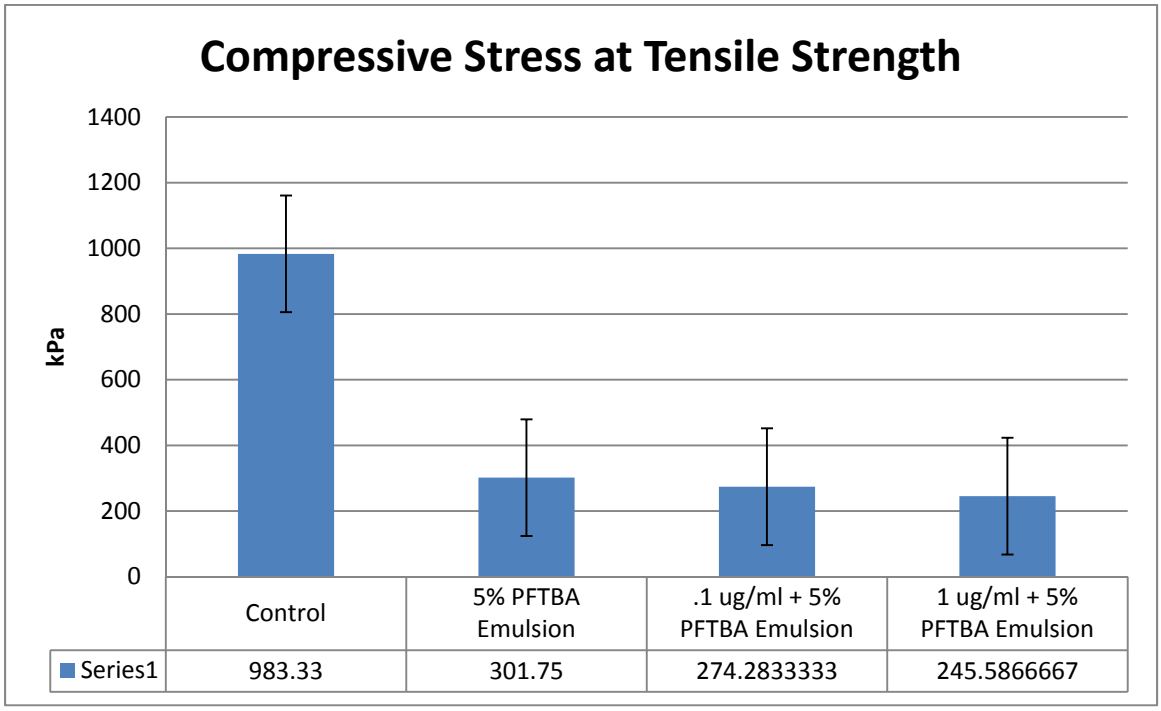

Figure 3.15: Compressive Stress of 3T3 laden hydrogels after 7 days. The control scaffold had significantly higher results than the remaining scaffolds. The remaining scaffolds decreased in results, with increasing concentration of SWCNTs.

3.8 Discussion

Three dimensional cell laden scaffolds are produced through the combination of three dimensional bio-plotters and printers, computer assisted design software, hydrogels, and various cell types. Cells are infused within hydrogels and are then extruded through tubing by the printer to produce computer designed structures. These structures are intended to be identical to their computer and organ models, however lack the necessary mechanical and chemical features to encourage cellular life once printed. Success with cellular scaffolds is due to proper selection of hydrogels and key additives in various concentrations. Single walled carbon nanotubes were chosen due to their ability to increase mechanical features in three dimensional scaffolds and other biomaterials. The incorporation of perfluorotributylamine was also used to increase cell viability due to various studies showing its success in tissue formation.

This study was conducted to determine the scaffold's structure as a function of alginate hydrogel with an added constant perfluorotributylamine concentration with increasing amounts of single walled carbon nanotubes.

Four scaffolds concentrations were produced, a alginate control with no single walled carbon nanotubes and no perfluorotributylamine, alginate with 5% by weight perfluorotributylamine, alginate with 5% by weight perfluorotributylamine and .1 μg/ml single walled carbon nanotubes, and alginate with 5% by weight perfluorotributylamine and 1 μg/ml single walled carbon nanotubes.

Working with the control and the three modified scaffolds, the results display high cell viability. Results show increased cell viability with the addition of the perfluorotributylamine emulsion and increase with increasing amounts of single walled carbon nanotubes. The increased cell viability in the scaffolds containing the perfluorotributylamine is believed to have occurred due to the increased oxygen content that is normally associated with the addition of perfluorotributylamine and also due to the imitated extracellular matrix produced by the single walled carbon nanotubes.

The mechanical properties are shown to decrease with the addition of perfluorotributylamine and continue to decrease as the carbon nanotube concentration is increased, correlating indirectly with the hypothesis. The poor mechanical properties in the alginate with 5% by weight perfluorotributylamine, alginate with 5% by weight perfluorotributylamine and .1 μg/ml single walled carbon nanotubes, and alginate with 5% by weight perfluorotributylamine and 1 μg/ml single walled carbon nanotubes scaffolds are hypothesized to be due to the addition of perfluorotributylamine. In future studies, adjusting the amount of perfluorotributylamine can potentially increase mechanical properties.

3.9 Conclusion

The utilization of three dimensional bio plotting provides an opportunity for researchers and engineers to create an alternative method to donor exact organ transplantation. This study explored the effect of different concentrations of single walled carbon nanotubes added in increasing amounts to a 5% perfluorotributylamine emulsion and concluded that the 5% by weight perfluorotributylamine emulsion and 1 μg/ml single walled carbon nanotube scaffold displayed the highest cell viability compared to the control, alginate with 5% by weight perfluorotributylamine, alginate with 5% by weight perfluorotributylamine and .1 μg/ml single walled carbon nanotube scaffolds. The control scaffold with a 0 concentration of both single walled carbon nanotubes and perfluorotributylamine emulsion displayed the optimal mechanical strength compared to the 5% by weight perfluorotributylamine, alginate with 5% by weight perfluorotributylamine and .1 μg/ml single walled carbon nanotubes, and alginate with 5% by weight perfluorotributylamine and 1 μg/ml single walled carbon nanotubes scaffolds. Based on these results further studies may prove beneficial to exploring a better combination of the proposed components to increase cell viability while also increasing or maintaining mechanical properties.

4. SUMMARY, CONCLUSIONS, AND RECOMMENDATIONS

4.1 Summary

Three dimensionally printed constructs are a stepping stone to the application of fully printed donor identical organs and tissues. The use of alginate hydrogels cross-linked with calcium chloride to form three dimensional shapes has been widely researched in literature, with various additives and configurations. Within this study of the additive benefits of carbon nanotubes and perfluorotributylamine into an alginate hydrogel structure formed via a three dimensional bioplotter, various combinations were produced with a potential to increase mechanical stability and cellular viability. This study is beneficial to the growing need for donor substitutions and patient identical constructs which will be immune compatible.
These scaffold configurations are similar to those widely used in various research programs where alginate is the base hydrogel.

To study the potential of this theory an in vitro study was conducted to test the cytocompatibility, mechanical properties, and the morphological effects on cells as a function of the configuration of a perfluorotributylamine addition to increasing concentrations of carbon nanotubes within alginate. The alginate only, 5% perfluorotributylamine + alginate, 5% perfluorotributylamine + .1 µg/ml carbon nanotube + alginate, and 5% perfluorotributylamine + 1 µg/ml carbon nanotube + alginate scaffolds underwent an live/dead assay, Picogreen assay, f-actin stain, and compression testing.

4.2 Conclusions

The results of this study indicate that the configuration of 5% perfluorotributylamine + 1 µg/ml carbon nanotube + alginate, provided the best cell viability results; Picogreen fluorescence of 8532, excellent viability in live/dead stain, and excellent morphological features. The control scaffold, containing alginate only, provided the best mechanical integrity compared to the other configurations. This provides more insight to the proper configuration between perfluorotributylamine and carbon nanotubes within an alginate scaffold to reach a non-toxic, mechanically stable structure. The Picogreen fluorescence of the scaffolds increased with increasing carbon nanotube concentration while mechanical properties decreased with increasing carbon nanotube concentration. Further research into effect on the morphological structure could be done.

4.3 Recommendations

1. Testing various other hydrogels and hydrogel configurations instead of alginate and calcium chloride as a cross linking solution with the perfluorotributylamine emulsion and single walled carbon nanotube configurations used in this study. This may lead to increased mechanical properties.
2. Testing the incorporation of various other types of perfluorocarbons instead of perfluorotributylamine to research their effect on the used configurations.
3. Testing the use of strictly perfluorotributylamine emulsion without any single walled carbon nanotubes.

4. Varying the amount of perfluorotributylamine emulsion and researching its effect on the previously used single walled carbon nanotube concentrations.
5. Tensile and fatigue testing could be done to better understand the mechanical limitations of the current models.
6. An in vivo study within an animal model could be conducted to get a real life application of the effects of mechanical strength and compatibility.
7. A study on the incorporation of adipose derived stem cells and their ability to differentiate into various cell lines within the various scaffold configurations.

REFERENCES

1. "3D bioprinting of tissues and organs" Sean V. Murphy & Anthony Atala, Nature biotechnology.

2. Hull, C.W. Apparatus for production of three-dimensional objects by stereolithography. US 4575330 A (Google Patents, 1986).

3. Ingber, D.E. et al. Tissue engineering and developmental biology: going biomimetic. Tissue Eng. 12, 3265–3283 (2006)
4. Derby, B. Printing and prototyping of tissues and scaffolds. Science 338, 921–926 (2012).

5. Kasza, K.E. et al. The cell as a material. Curr. Opin. Cell Biol. 19, 101–107 (2007).

6. Mironov, V. et al. Organ printing: tissue spheroids as building blocks. Biomaterials 30, 2164–2174 (2009).

7. Kelm, J.M. et al. A novel concept for scaffold-free vessel tissue engineering: self-assembly of microtissue building blocks. J. Biotechnol. 148, 46–55 (2010).

8. Kamei, M. et al. Endothelial tubes assemble from intracellular vacuoles in vivo. Nature 442, 453–456 (2006).

9. Alajati, A. et al. Spheroid-based engineering of a human vasculature in mice. Nat. Methods 5, 439–445 (2008).

10. Jones, N. Science in three dimensions: the print revolution. Nature 487, 22–23 (2012).

11. Khalil, S. & Sun, W. Biopolymer deposition for freeform fabrication of hydrogel tissue constructs. Mater. Sci. Eng. C 27, 469–478 (2007).

12. Cohen, D.L., Malone, E., Lipson, H. & Bonassar, L.J. Direct freeform fabrication of seeded hydrogels in arbitrary geometries. Tissue Eng. 12, 1325–1335 (2006).

13. Jakab, K., Damon, B., Neagu, A., Kachurin, A. & Forgacs, G. Three-dimensional tissue constructs built by bioprinting. Biorheology 43, 509–513 (2006).

14. Chang, C.C., Boland, E.D., Williams, S.K. & Hoying, J.B. Direct-write bioprinting three-dimensional biohybrid systems for future regenerative therapies. J. Biomed. Mater. Res. B Appl. Biomater. 98, 160–170 (2011).

15. Smith, C.M. et al. Three-dimensional bioassembly tool for generating viable tissue engineered constructs. Tissue Eng. 10, 1566–1576 (2004).

16. Chang, R., Nam, J. & Sun, W. Effects of dispensing pressure and nozzle diameter on cell survival from solid freeform fabrication-based direct cell writing. Tissue Eng. Part A 14, 41–48 (2008).

17. Skardal, A., Zhang, J., McCoard, L., Oottamasathien, S. & Prestwich, G.D. Dynamically crosslinked gold nanoparticle—hyaluronan hydrogels. Adv. Mater. 22, 4736–4740 (2010).

18. Skardal, A. et al. Photocrosslinkable hyaluronan-gelatin hydrogels for two-step bioprinting. Tissue Eng. Part A 16, 2675–2685 (2010).

19. U.S. Department of Health and Human Service. Donate the gift of life. Available from: www.organdonor.gove/index.html (Accessed March 9, 2015).

20. Drury, Jeanie L., and David J. Mooney. "Hydrogels for Tissue Engineering: Scaffold Design Variables and Applications." *Biomaterials* 24.24 (2003): 4337-351. Web.

21. Park JB, Lakes RS. Biomaterials: an introduction, 2nd ed. New York: Plenum Press; 1992.

22. Smidsr^d O, Skjak-Bræk G. Alginate as immobilization matrix (for cells. Trends Biotech 1990;8:71–8.

23. Johnson FA, Craig DQM, Mercer AD. Characterization of the block structure and molecular weight of sodium alginates. J Pharm Pharmacol 1997;49:639–43.

24. Draget KI, Strand B, Hartmann M, Valla S, Smidsr^d O, Skjak- (Brck G. Ionic and acid gel formation of epimerised alginates: the ! effect of AlgE4. Int J Biol Macromol 2000;27:117–22.

25. LeRoux MA, Guilak F, Setton LA. Compressive and shear properties of alginate gel: effects of sodium ions and alginate concentration. J Biomed Mater Res 1999;47:46–53.

26. Hopley, Erin Leigh, Shima Salmasi, Deepak M. Kalaskar, and Alexander M. Seifalian. "Carbon Nanotubes Leading the Way Forward in New Generation 3D Tissue Engineering." *Biotechnology Advances* 32.5 (2014): 1000-014. Web.

27. De Volder MF, Tawflick SH, Baughman RH, Hart AJ. Carbon nanotubes: present and future commercial applications. Science 2013;399(6119):535–9. [1].

28. Arjmandi N, Sasanpour P, Rashidian B. CVD synthesis of small-diameter single-walled carbon nanotubes on silicon. Comput Sci Eng Electr Eng 2009;16(1):61–4.

29. Demczyk BG, Wang YM, Cumings J, Hetman M, Han W, Zettl A, et al. Direct mechanical measurement of tensile strength and elastic modulus of mutliwalled carbon nanotubes. Mater Sci Eng 2002;334:173–8.

30. Yu MF, Files SB, Arepalli S, Ruoff RS. Tensile loading of ropes of single wall carbon nanotubes and their mechanical properties. Phys Rev Lett 2000;84:5552–5.

31. Qian D, Dickey EC, Andrews R, Rantell T. Load transfer and deformation mechanisms in carbon nanotubepolystyrene composites. Appl Phys Lett 2000;76:2868–70.

32. Mackle J, Blond D, Mooney E, McDonnell C, Blau W, Shaw G, et al. In vitro characterization of an electroactive carbon-nanotube-based nanofiber scaffold for tissue engineering. Macromol Biosci 2011;11:1272–82.

33. Cheng Q, Rutledge K, Jabbarzadeh E. Carbon nanotube-poly(lactide-co-glycolide) composite scaffolds for bone tissue engineering applications. Ann Biomed Eng 2013;41: 904–16.

34. Coleman JN, Khan U, Blau WJ, Gun'ko YK. Small but strong: a review of the mechanical properties of carbon nanotube-polymer composites. Carbon 2006;44:1624–52.

35. Armentano I, Dottori M, Fortunati E, Mattioli S, Kenny JM. Biodegradable polymer matrix nanocomposites for tissue engineering: A review. Polymer Degradation and Stability 2010;95(11):2126–46.

36. Zanello LP, Zhao B, Hu H, Haddon RC. Bone cell proliferation on carbon nanotubes. Nano Lett 2006;6:562–7.

37. Namgung S, Baik KY, Park J, Hong S. Controlling the growth and differentiation of human mesenchymal stem cells by the arrangement of individual carbon nanotubes. ACS Nano 2011;5:7383–90.

38. Gheith MK, Pappas TC, Liopo AV, Sinani VA, Shim BS, Motamedi M, et al. Stimulation of neural cells by lateral currents in conductive layer-by-layer films of single-walled carbon nanotubes. Adv Mater 2006;18:2975–9.

39. A, Valiani, Hashemibeni B, Esfandiary E, Moradi I, and Narimani M. "The Evaluation of Toxicity of Carbon Nanotubes on the Human Adipose-derived-stem Cells In-vitro." *Advanced Biomedical Research Adv Biomed Res* 3.1 (2014): 40. Web.

40. A, Valiani, Hashemibeni B, Esfandiary E, Ansar M, Kazemi M, and Nafiseh E. "Study of Carbon Nano-Tubes Effects on the Chondrogenesis of Human Adipose Derived Stem Cells in Alginate Scaffold." *International Journal of Preventive Medicine* 5.7 (2014): 825-834. Web.

41. Zhao B, Hu H, Mandal SK, Haddon RC. A bone mimic based on the self-assembly of hydroxyapatite on chemically functionalized single-walled carbon nanotubes. Chem Mater 2005;17:3235–41.

42. Balasubramanian K, Burghard M. Chemically functionalized carbon nanotubes. Small 2005;1(2):180–92.

43. Newman P, Minett A, Ellis-Behnke R, Zreiqat H. Carbon nanotubes: Their potential and pitfalls for bone tissue regeneration and engineering. Nanomedicine 2013;9: 1139–58.

44. Chahine NO, Collette N, Thomas C, Genetos DC, Loots GG. Nanocomposite scaffold for chondrocyte growth and cartilage tissue engineering: effects of carbon nanotube surface functionalisation. Tissue Eng Part A 2014.

45. Madani SY, Tan A, Dwek M, Seifalian AM. Functionalization of single-walled carbon nanotubes and their binding to cancer cells. Int J Nanomedicine 2012;7:905–14. http://dx. doi.org/10.2147/IJN.S25035.

46. Lowe, Kenneth C., Michael R. Davey, and J.brian Power. "Perfluorochemicals: Their Applications and Benefits to Cell Culture." *Trends in Biotechnology* 16.6 (1998): 272-77. Web.

47. Cho, Moo H., and Shaw S. Wang. "Enhancement of Oxygen Transfer in Hybridoma Cell Culture by Using a Perfluorocarbon as an Oxygen Carrier." *Biotechnology Letters Biotechnol Lett* 10.12 (1988): 855-60. Web.

48. Ju, Lu Kwang, Jaw F. Lee, and William B. Armiger. "Enhancing Oxygen Transfer in Bioreactors by Perfluorocarbon Emulsions." *Biotechnol. Prog. Biotechnology Progress* 7.4 (1991): 323-29. Web.

49. Campos, Daniela F Duarte, Andreas Blaeser, Michael Weber, Jörg Jäkel, Sabine Neuss, Wilhelm Jahnen-Dechent, and Horst Fischer. "Three-dimensional Printing of Stem Cell-laden Hydrogels Submerged in a Hydrophobic High-density Fluid." *Biofabrication* 5.1 (2012): 015003. Web.

50. Benjamin, Shimon, Dmitriy Sheyn, Shiran Ben-David, Anthony Oh, Ilan Kallai, Ning Li, Dan Gazit, and Zulma Gazit. "Oxygenated Environment Enhances Both Stem Cell Survival and Osteogenic Differentiation." *Tissue Engineering Part A* 19.5-6 (2013): 748-58. Web.

51. Ma, Teng, Yuqing Wang, Fengyu Qi, Shu Zhu, Liangliang Huang, Zhongyang Liu, Jinghui Huang, and Zhuojing Luo. "The Effect of Synthetic Oxygen Carrier-enriched Fibrin Hydrogel On Schwann Cells under Hypoxia Condition In vitro." *Biomaterials* 34.38 (2013): 10016-0027. Web.

52. Kimelman-Bleich, Nadav, Gadi Pelled, Dima Sheyn, Ilan Kallai, Yoram Zilberman, Olga Mizrahi, Yamit Tal, Wafa Tawackoli, Zulma Gazit, and Dan Gazit. "The Use of a Synthetic Oxygen Carrier-enriched Hydrogel to Enhance Mesenchymal Stem Cell-based Bone Formation in Vivo." *Biomaterials* 30.27 (2009): 4639-648. Web.

53. Chin, S.-F., R. H. Baughman, A. B. Dalton, G. R. Dieckmann, R. K. Draper, C. Mikoryak, I. H. Musselman, V. Z. Poenitzsch, H. Xie, and P. Pantano. "Amphiphilic Helical Peptide Enhances the Uptake of Single-Walled Carbon Nanotubes by Living Cells." *Experimental Biology and Medicine* 232.9 (2007): 1236-244. Web.

VITA

Joshua Tate is the son of Delvin P. Tate and Stephanie M. Tate of Zachary, Louisiana. He received his Bachelors of Science degree in Biological Engineering at Louisiana State University in 2012. In the fall of 2013, he enrolled in the Biological Engineering Master's program at Louisiana State University under Dr. Daniel Hayes. He plans to further pursue industry work in the biomedical engineering field with entrepreneurial aspirations.